

# Franconite, $\text{NaNb}_2\text{O}_5(\text{OH})\cdot 3\text{H}_2\text{O}$ : structure determination and the role of H bonding, with comments on the crystal chemistry of franconite-related minerals

M. M. M. HARING\* AND A. M. McDONALD

Department of Earth Sciences, Laurentian University, Sudbury, Ontario P3E 2C6, Canada

[Received 30 November 2013; Accepted 11 February 2014; Associate Editor: E. Grew]

## ABSTRACT

The crystal structure of franconite,  $\text{NaNb}_2\text{O}_5(\text{OH})\cdot 3\text{H}_2\text{O}$ , has been characterized by single-crystal X-ray diffraction using material from Mont Saint-Hilaire, Québec, Canada. Results give  $a = 10.119(2)$ ,  $b = 6.436(1)$ ,  $c = 12.682(2)$  Å and  $\beta = 99.91(3)^\circ$  and confirm the correct space group as  $P2_1/c$ . The crystal structure, refined to  $R = 4.63\%$  and  $wR^2 = 11.95\%$ , contains one *Na* site, two distorted octahedral *Nb* sites and nine *O* sites. It consists of clusters of four edge-sharing  $\text{Nb}(\text{O},\text{OH})_6$  octahedra, linked through shared corners to adjacent clusters, forming layers of  $\text{Nb}(\text{O},\text{OH})_6$  octahedra. These alternate along [100] with layers composed of  $\text{NaO}(\text{H}_2\text{O})_4$  polyhedra, the two being linked together by well defined H bonding. The predominance of H bonding, essential to the mineral, results in a perfect {100} cleavage. Chemical analyses ( $n = 7$ ) of four crystals give the empirical formula  $(\text{Na}_{0.73}\text{Ca}_{0.13}\square_{0.14})_{\Sigma=1.00}(\text{Nb}_{1.96}\text{Ti}_{0.02}\text{Si}_{0.02}\text{Al}_{0.01})_{\Sigma=2.01}\text{O}_5(\text{OH})\cdot 3\text{H}_2\text{O}$  (based on nine oxygens) or ideally  $\text{NaNb}_2\text{O}_5(\text{OH})\cdot 3\text{H}_2\text{O}$ . Franconite is crystallo-chemically related to SOMS [Sandia Octahedral Molecular Sieves;  $\text{Na}_2\text{Nb}_{2-x}\text{M}_x\text{O}_{6-x}(\text{OH})_x\cdot \text{H}_2\text{O}$  with  $\text{M} = \text{Ti}, \text{Zr}, \text{Hf}$ ], a group of synthetic compounds with strong ion-exchange capabilities. Both hochelagaite ( $\text{CaNb}_4\text{O}_{11}\cdot n\text{H}_2\text{O}$ ) and ternovite ( $\text{MgNb}_4\text{O}_{11}\cdot n\text{H}_2\text{O}$ ) have X-ray powder diffraction patterns and cation ratios similar to those of franconite indicating that these minerals probably have similar structures.

**KEYWORDS:** franconite, hochelagaite, ternovite, crystal structure, Mont Saint-Hilaire, hydrogen bonding.

## Introduction

FRANCONITE,  $\text{NaNb}_2\text{O}_5(\text{OH})\cdot 3\text{H}_2\text{O}$ , is the Na-dominant endmember of a ternary system with other hydrated Nb oxides including hochelagaite ( $\text{CaNb}_4\text{O}_{11}\cdot n\text{H}_2\text{O}$ ; Jambor *et al.*, 1986) and ternovite ( $\text{MgNb}_4\text{O}_{11}\cdot n\text{H}_2\text{O}$ ; Subbotin *et al.*, 1997). The mineral was first discovered at the Francon quarry in the St-Michel district of Montreal, Québec where it occurs in vugs within dawsonite-bearing sills as white polycrystalline globules (average diameter  $\sim 0.15$  mm) consisting of radiating, extremely thin, blades (average dimensions =  $0.030$  mm  $\times$   $0.005$  mm

$\times 0.001$  mm; Jambor *et al.*, 1986). It has also been discovered in other agpaitic environments including Mont Saint-Hilaire (Horváth and Gault, 1990), the Saint-Amable sill (Horváth *et al.*, 1998), the Khibiny massif (Pekov and Podlesnyi, 2004), the Vuoriyarvi alkaline-ultrabasic massif (Belovitskaya and Pekov, 2004) and the Vishnevogorsk alkali complex (Nikandrov, 1990). In the original description, Jambor *et al.* (1984) gave a unit cell of  $a = 22.22(1)$ ,  $b = 12.857(5)$ ,  $c = 6.359(4)$  Å and  $\beta = 92.24(6)^\circ$ . Data from chemical analyses indicated the ideal formula  $\text{Na}_2\text{Nb}_4\text{O}_{11}\cdot n\text{H}_2\text{O}$  ( $n = 8-9$ ) but with variable Na:Ca ratios, as well as trace Ti, Al, Si and Sr (Jambor *et al.*, 1984). It is quite likely that the variable Na:Ca ratios are a function of both franconite and hochelagaite being found together

\* E-mail: mx\_haring@laurentian.ca  
DOI: 10.1180/minmag.2014.078.3.09

in the same complex globules, an observation made during this current study. The two minerals also have similar optical properties, making them indistinguishable megascopically (Jambor *et al.*, 1984, 1986).

To date, only X-ray powder diffraction (XRPD) studies have been completed on franconite as the small crystal size of the mineral has precluded analysis by typical single-crystal methods. As such, the true chemical formula and crystal structure of the mineral have remained largely unknown. With the introduction of extremely bright X-ray sources arising from a combination of rotating-anode generators coupled with multi-layer optics, incident-beam paths and highly sensitive detectors, it is now possible to study the crystal structures of minerals (Cooper and Hawthorne, 2012) such as franconite. In this study results are reported from a successful single-crystal study of franconite, a description of its structure is presented and the complex nature of H bonding within franconite is described, along with comments on the significance of the crystal structure in the context of the chemical variation in franconite and the related minerals: hochelagaite and ternovite. As franconite is a late-stage mineral occurring in many agpaite environments, understanding its crystal structure can help to better understand processes related to the low-temperature alteration of Nb-rich minerals.

### Occurrence and description

The franconite used in this study was collected at the Poudrette quarry, La Vallée-du-Richelieu,

Montérégie (formerly Rouville County), Québec, Canada, where it occurs as a rare mineral in sodalite-syenite, miarolitic cavities and hornfels microenvironments (Horvath and Gault, 1990). The material used in this study came from sodalite-syenite where it occurs in association with microcline, analcime, sodalite, siderite and pyrite (Table 1). Franconite occurs in spherical aggregates of radiating bladed crystals that are ~0.15–0.20 mm in diameter. Individual crystals of franconite are, on average, 0.008 mm × 0.020 mm × 0.060 mm, euhedral, with a perfect {100} cleavage and they display the forms pinacoid {100} and {011}.

### Chemistry

Chemical analyses of franconite were performed with a JEOL JSM 6400 scanning electron microscope using a voltage of 20 kV, a beam current of ~1 nA and a beam width of 1 µm. Data from energy-dispersive spectrometry (EDS) were collected using the following standards (X-ray lines): CaTiO<sub>3</sub> (CaK $\alpha$ , TiK $\alpha$ ), synthetic MnNb<sub>2</sub>O<sub>6</sub> (NbK $\alpha$ ) and albite (NaK $\alpha$ , SiK $\alpha$ , AlK $\alpha$ ). The globules analyzed in this study were found to contain crystals of near endmember franconite, along with compositions intermediate between franconite and hochelagaite (i.e. with variable Na:Ca ratios) and near endmember hochelagaite. None of the crystals appears to be chemically zoned when viewed perpendicular to the layering. Due to the variation of Na and Ca in the globules of franconite, 15 separate crystals were isolated for chemical analysis. Of these, four were found

TABLE 1. Modal abundances and descriptions of minerals associated with franconite.

Mineral	Modal abundance (%)	Description
Microcline (KAlSi <sub>3</sub> O <sub>8</sub> )	~45	Light grey subhedral crystals ranging from ~2 to 5 mm in diameter.
Analcime Na <sub>2</sub> (Al <sub>2</sub> Si <sub>4</sub> O <sub>12</sub> )·2H <sub>2</sub> O	~25	Translucent, anhedral to subhedral crystals ranging from 2 to 3 mm in diameter.
Sodalite Na <sub>8</sub> (Al <sub>6</sub> Si <sub>6</sub> O <sub>24</sub> )Cl <sub>2</sub>	~15	Light blue anhedral crystals ranging from 1 to 3 mm in diameter.
Siderite FeCO <sub>3</sub>	~10	Light brown to tan euhedral crystals exhibiting the form rhombohedron {10 $\bar{1}$ 1} and ranging from 3 to 5 mm in diameter
Pyrite FeS <sub>2</sub>	~5	Anhedral crystals ranging from 1 to 3 mm in diameter

to have franconite-rich compositions, with the remaining ones having either hochelagaite-rich or intermediate franconite–hochelagaite compositions. Chemical analyses ( $n = 7$ ) of the four franconite-rich crystals give the average (range) composition (wt.%): Na<sub>2</sub>O 6.45 (5.03–8.87), CaO 2.00 (0.34–3.27), Nb<sub>2</sub>O<sub>5</sub> 74.23 (72.50–75.43), TiO<sub>2</sub> 0.52 (0.40–0.75), SiO<sub>2</sub> 0.42 (0.27–0.81), Al<sub>2</sub>O<sub>3</sub> 0.11 (0.04–0.27) and H<sub>2</sub>O (calc.) 17.96 and total = 101.69, corresponding to the empirical formula: (Na<sub>0.73</sub>Ca<sub>0.13</sub>□<sub>0.14</sub>)<sub>Σ=1.00</sub>(Nb<sub>1.96</sub>Ti<sub>0.02</sub>Si<sub>0.02</sub>Al<sub>0.01</sub>)<sub>Σ=2.01</sub>O<sub>5</sub>(OH)·3H<sub>2</sub>O (based on 9 oxygens) or ideally NaNb<sub>2</sub>O<sub>5</sub>(OH)·3H<sub>2</sub>O. Although the Na site was determined to be fully occupied in the crystal-structure refinement, the empirical formula indicates a minor deficiency in the Na site, a feature that may be explained by the instability of the mineral and possible migration of Na under the electron beam. The ideal formula originally proposed for franconite by Jambor *et al.* (1984) was Na<sub>2</sub>Nb<sub>4</sub>O<sub>11</sub>· $n$ H<sub>2</sub>O, determined on the basis of ΣNb+Ti+Si+Al = 4, as the nature of the anions was unclear. The ideal formula proposed here is derived from results of the crystal-structure analysis and to a greater extent, more clearly defines the content and roles of (OH) and H<sub>2</sub>O in the mineral. In light of the obvious chemical variation that may exist in franconite, data from wavelength-dispersive spectrometry (WDS) were also collected on the crystal used for the single-crystal X-ray structure study. These were obtained using a Cameca SX-100 electron microprobe operated with an excitation voltage of 15 kV, 5 nA current and a 15 μm beam width (chosen to reduce migration of Na). The following standards (X-ray lines) were used: albite (NaKα), olivine (MgKα), diopside (CaKα, SiKα), andalusite (AlKα), titanite (TiKα), Ba<sub>2</sub>NaNb<sub>5</sub>O<sub>15</sub> (NbKα) and SrTiO<sub>3</sub> (SrKα). The compositions of two points taken from the crystal used for single-crystal analysis are similar to those presented above, confirming the data obtained by energy-dispersive spectrometry. Data from the two data points obtained by WDS give the average composition: Na<sub>2</sub>O 7.60, CaO 0.35, Nb<sub>2</sub>O<sub>5</sub> 75.05, TiO<sub>2</sub> 0.61, SiO<sub>2</sub> 0.02, Al<sub>2</sub>O<sub>3</sub> 0.03 and H<sub>2</sub>O (calc.) 16.31 total 100%.

Other elements were sought but were not found to be present in statistically meaningful concentrations. In particular, data from EDS and WDS indicate franconite is devoid of Ta, an interesting observation considering the strong geochemical coupling behaviour between Nb and Ta

(Babechuk and Kamber 2011). Both Nb and Ta share crystal-chemical similarities such as identical charges (3+, 5+) as well as similar ionic radii (~0.64 Å for <sup>61</sup>Nb<sup>5+</sup> and <sup>61</sup>Ta<sup>5+</sup>; Shannon *et al.* 1976), so would be predicted to substitute readily for one another in crystal structures. Niobium-bearing minerals such as vuonnemite [Na<sub>11</sub>Ti<sup>4+</sup>Nb<sub>2</sub>(Si<sub>2</sub>O<sub>7</sub>)<sub>2</sub>(PO<sub>4</sub>)<sub>2</sub>O<sub>3</sub>(F,OH); Ercit *et al.*, 1998], epistolite [Na<sub>4</sub>Nb<sub>2</sub>Ti<sup>4+</sup>(Si<sub>2</sub>O<sub>7</sub>)<sub>2</sub>O<sub>2</sub>(OH)<sub>2</sub>(H<sub>2</sub>O)<sub>4</sub>; Sokolova and Hawthorne, 2004] and laurentianite {[NbO(H<sub>2</sub>O)]<sub>3</sub>(Si<sub>2</sub>O<sub>7</sub>)<sub>2</sub>[Na(H<sub>2</sub>O)<sub>2</sub>]<sub>3</sub>; Haring *et al.*, 2012} from alkaline environments similar to those in which franconite forms, also exhibit a virtual absence of Ta. These observations may suggest a possible fractionation between Nb and Ta occurring prior to the formation of these minerals, which would also hold for franconite. The exact cause of the Nb-Ta decoupling mechanism remains unknown, but given that it is observed in Nb-bearing minerals from a number of agpaitic environments, the implication is that it must be related to the geochemical processes leading to the formation of these unusual lithologies.

### Raman and infrared spectroscopy

Raman and infrared spectroscopy of franconite was carried out to investigate the presence of OH and H<sub>2</sub>O. The Raman spectrum of franconite was collected using a Horiba Jobin Yvon XPLORA Raman spectrometer interfaced with an Olympus BX41 microscope over a range of 50–4000 cm<sup>-1</sup>. The spectrum (Fig. 1) represents an average of three spectra, each collected with 20 s acquisition cycles. An excitation radiation of λ = 638 nm was used, along with a 600 grating and 100× magnification (producing a beam of diameter = 2 μm). The excitation radiation of λ = 638 nm was chosen to eliminate fluorescence peaks in the region of ~2000–2500 cm<sup>-1</sup> which were observed when spectra were collected using λ = 532 nm. Calibration was undertaken using the 521 cm<sup>-1</sup> line of a Si wafer. The Raman spectrum of franconite contains bands in two regions: at ~212–924 and 3416 cm<sup>-1</sup> (Fig. 1). The first consists of sharp, moderate to high intensity peaks at 212, 297, 391, 461, 583, 661, 879 and 924 cm<sup>-1</sup>. Those peaks occurring below 500 cm<sup>-1</sup> are associated with Na–O/Ca–O bonding (Table 2). The remaining high-intensity peaks are attributed to the two distinct distorted octahedral sites associated with Nb (see below). Those peaks attributed to Nb–O were assigned

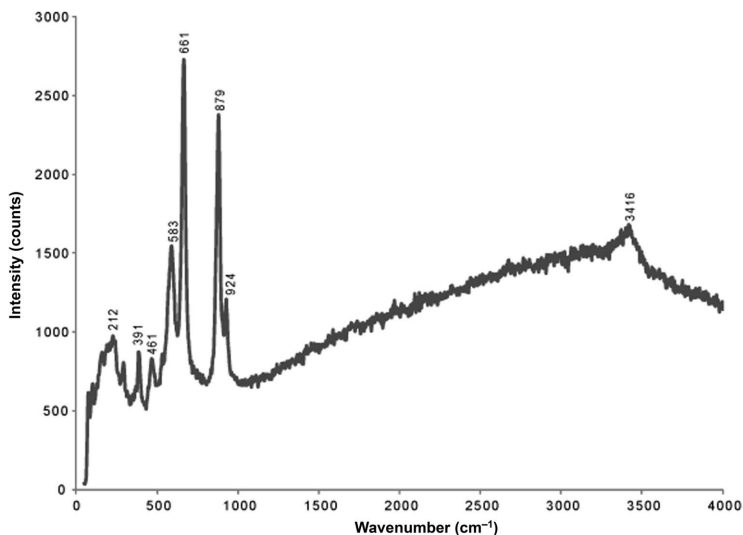


FIG. 1. Raman spectrum of franconite.

based on data on Nb oxides presented by Jehng and Wachs (1990). Peaks at 583 and 661  $\text{cm}^{-1}$  are attributed to symmetric stretching of the Nb–O–Nb linkages associated with two crystallographically independent  $\text{Nb}(\text{O},\text{OH})_6$  octahedra (Fig. 1). The peaks at 879 and 924  $\text{cm}^{-1}$  are attributed to symmetric stretching of possible Nb=O bonds present in the distorted  $\text{Nb}(\text{O},\text{OH})_6$  sites (Jehng and Wachs, 1990). The final Raman band is a single, broad, low intensity peak at 3416  $\text{cm}^{-1}$  associated with O–H stretching (Williams, 1995). The Raman spectra of the synthetic phases  $\text{HCa}_2\text{Nb}_3\text{O}_{10}$  and  $\text{KCa}_2\text{Nb}_3\text{O}_{10}$  (Jehng and Wachs, 1990) as well as those of SOMS [Sandia Octahedral Molecular Sieves;

$\text{Na}_2\text{Nb}_{2-x}\text{M}_x\text{O}_{6-x}(\text{OH})_x\text{H}_2\text{O}$  with  $\text{M} = \text{Ti}, \text{Zr}, \text{Hf}$ ; Nyman *et al.*, 2002; Iliev *et al.*, 2003], are similar to that of franconite. The spectra of the synthetic phases both have a single, moderately strong Raman band in the region of  $\sim 750\text{--}800\text{ cm}^{-1}$ , associated with symmetric stretching of Nb=O bonds, as well as two moderately strong Raman bands in the region of  $450\text{--}650\text{ cm}^{-1}$ , associated with Nb–O–Nb linkages from two crystallographically independent  $\text{NbO}_6$  sites (Jehng and Wachs, 1990). In the region  $1200\text{--}1700\text{ cm}^{-1}$ , bands associated with H–O–H stretching could not be detected using Raman spectroscopy, probably because of the weak Raman scattering abilities of water.

TABLE 2. Observed absorption bands and band assignments for the Raman spectrum of franconite.

Raman absorption band ( $\text{cm}^{-1}$ )	Suggested assignment
3416	O–H stretching
924	Symmetric stretching of Nb=O double bond
879	Symmetric stretching of Nb=O double bond
661	Nb–O–Nb linkages – symmetric stretching
583	Nb–O–Nb linkages – symmetric stretching
461	Na–O/Ca–O
391	Na–O/Ca–O
297	Na–O/Ca–O
212	Na–O/Ca–O

## CRYSTAL CHEMISTRY OF FRANCONITE

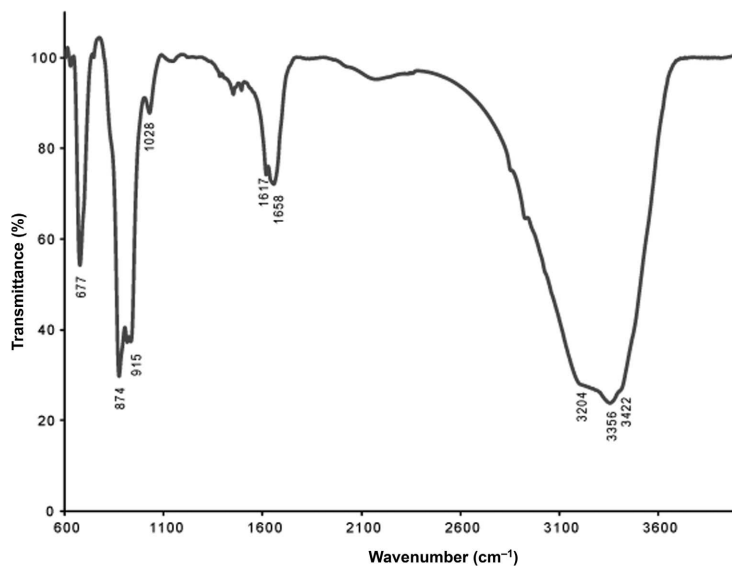


FIG. 2. FTIR spectrum of franconite with transmittance peaks indicated.

To confirm the presence of water in franconite and in light of the fact that water is a weak Raman scatterer but a strong absorber of infrared radiation, an infrared (FTIR) spectrum over the range 600–4000  $\text{cm}^{-1}$  was collected using a Bruker Alpha spectrometer equipped with a KBr beam splitter and a DTGS detector. This spectrum (Fig. 2), obtained by averaging 128 scans with a resolution of 4  $\text{cm}^{-1}$ , reveals four distinct bands at  $\sim 677 \text{ cm}^{-1}$ , 874–1028  $\text{cm}^{-1}$ , 1658  $\text{cm}^{-1}$  and 3204–3422  $\text{cm}^{-1}$ . Overall, the spectrum is similar to that reported by Jambor *et al.* (1984) and, with the exception of an additional band in the region of 1658  $\text{cm}^{-1}$ , the FTIR and Raman

spectra of franconite are identical. The first two regions at  $\sim 677 \text{ cm}^{-1}$  and 874–1028  $\text{cm}^{-1}$  are similar to those in the Raman spectrum at 563, 646, 815 and 877  $\text{cm}^{-1}$ ; these are attributed to the symmetric stretching of Nb–O–Nb and vibrations of terminal Nb=O bonds, respectively (Table 3; Fielicke *et al.*, 2003). The third region, centered at  $\sim 1658 \text{ cm}^{-1}$ , consists of a strong band at  $\sim 1658 \text{ cm}^{-1}$  with a shoulder at  $\sim 1617 \text{ cm}^{-1}$  and is attributed to H–O–H bending (Williams, 1995). The fourth region, at  $\sim 3204\text{--}3422 \text{ cm}^{-1}$ , is consistent with the weak Raman band at 3303  $\text{cm}^{-1}$  and consists of a strong band at  $\sim 3356 \text{ cm}^{-1}$  with shoulders at

TABLE 3. Observed transmittance bands and band assignments for the FTIR spectrum of franconite.

FTIR transmittance band ( $\text{cm}^{-1}$ )	Suggested assignment
3422	O–H stretching
3356	O–H stretching
3204	O–H stretching
1658	H–O–H stretching
1617	H–O–H stretching
1028	Nb=O double bond
915	Nb=O double bond
874	Nb=O double bond
677	Nb–O–Nb linkages – symmetric stretching

$\sim 3204$  and  $\sim 3422$   $\text{cm}^{-1}$  and is associated with O–H bending. A similar FTIR spectrum is observed for ternovite  $(\text{Mg,Ca})\text{Nb}_4\text{O}_{11}\cdot n\text{H}_2\text{O}$  (Subbotin *et al.*, 1997), implying that the mineral has crystal-chemical properties similar to those of franconite.

### X-ray crystallography and crystal-structure determination

X-ray powder diffraction data were collected using a 114.6 mm diameter Gandolfi camera, 0.3 mm collimator and Fe-filtered  $\text{CoK}\alpha$  radiation ( $\lambda = 1.7902$  Å). Intensities were determined using a scanned image of the powder pattern and normalized to the measured intensity of  $d = 9.968$  Å ( $I = 100$ ). The measured intensities were compared to a pattern calculated using results from the crystal-structure analysis and the program *CRYSCON* (Dowty, 2002) to determine how much an  $hkl$  plane contributed to a reflection. Overall, there is a good agreement between the measured and calculated powder patterns

(Table 4). The XRPD data for franconite in this study are broadly similar to those of Jambor *et al.* (1984); however, the highest intensity line in this study occurs at a  $d$  spacing of  $\sim 10$  Å rather than  $\sim 11$  Å as observed by Jambor *et al.* (1984). X-ray powder diffraction data from desiccated franconite ( $\text{Na}_2\text{Nb}_4\text{O}_{11}\cdot 3\text{H}_2\text{O}$ ) collected by Jambor *et al.* (1984) showed a strong line occurring at a  $d$  spacing of  $\sim 10$  Å, similar to franconite in the present study. Subsequent re-runs of the desiccated franconite over a 2 y period resulted in XRPD data showing a doublet at a  $d$  spacing of  $\sim 10$ – $11$  Å due to a gradual rehydration of franconite (Jambor *et al.*, 1984). These differences in hydration state may explain why the highest intensity line for franconite from this study has different  $d$  spacings from that given by Jambor *et al.* (1984).

To obtain a crystal for the next stage of the study, individual crystals were separated from a coarse-grained, franconite-bearing globule. These were examined optically and one of dimensions  $0.08$  mm  $\times$   $0.02$  mm  $\times$   $0.01$  mm, exhibiting a

TABLE 4. Franconite X-ray powder diffraction data.

$I_{\text{meas}}$	$I_{\text{calc}}$	$d_{\text{meas}}$ (Å)	$d_{\text{calc}}$ (Å)	$h$	$k$	$l$	$I_{\text{meas}}$	$I_{\text{calc}}$	$d_{\text{meas}}$ (Å)	$d_{\text{calc}}$ (Å)	$h$	$k$	$l$
100	100	10.211	9.968	1	0	0	5	1	2.114	2.112	1	0	$\bar{6}$
3	7	6.261	6.246	0	0	$\bar{2}$		2		2.097	1	3	0
23	16	5.479	5.407	1	1	0	5	1	2.044	2.029	0	3	$\bar{2}$
21	6	5.050	4.984	2	0	0	9	3	2.007	2.002	5	0	$\bar{2}$
	16		4.925	1	0	2		1		1.998	3	1	4
6	5	4.265	4.271	2	0	$\bar{2}$		1		1.994	5	0	0
15	11	3.989	3.941	2	1	0	5	5	1.985	1.971	1	0	6
	2		3.914	2	1	$\bar{1}$	4	2	1.918	1.911	5	1	$\bar{2}$
	7		3.911	1	1	2	2	2	1.903	1.904	5	1	0
3	2	3.693	3.619	2	1	1	6	2	1.779	1.776	3	3	$\bar{2}$
	3		3.605	2	0	2	2	1	1.764	1.766	1	2	$\bar{6}$
6	6	3.560	3.556	2	1	$\bar{2}$		1		1.761	3	3	1
21	15	3.213	3.218	0	2	0	2	1	1.730	1.736	2	3	3
32	14	3.157	3.145	2	1	2		2		1.736	4	1	4
	12		3.138	1	0	$\bar{4}$	5	1	1.708	1.713	1	3	4
	13		3.123	0	0	$\bar{4}$		2		1.7	5	2	$\bar{2}$
9	6	3.097	3.116	0	2	$\bar{1}$		1		1.695	5	2	0
16	19	2.843	2.843	3	1	$\bar{2}$	3	3	1.683	1.692	4	1	$\bar{6}$
3	1	2.725	2.704	2	2	0		2		1.69	3	3	2
3	2	2.629	2.628	2	1	$\bar{4}$		2		1.681	1	2	6
6	1	2.578	2.57	2	2	$\bar{2}$	5	1	1.597	1.596	0	4	$\bar{1}$
2	4	2.520	2.524	3	1	2	2	1	1.567	1.569	2	0	$\bar{8}$
4	6	2.303	2.302	4	1	$\bar{2}$	1	1	1.527	1.525	2	1	$\bar{8}$
6	2	2.262	2.247	1	2	$\bar{4}$							
	2		2.241	0	2	$\bar{4}$							

simple extinction and no evidence of twinning, was selected. X-ray intensity data were collected on a Bruker D8 three-circle diffractometer equipped with a rotating-anode generator, multi-layer optics incident beam path and an APEX-II CCD detector. X-ray diffraction data (28,653 reflections) were collected to  $60^\circ 2\theta$  using 20 s per  $0.3^\circ$  frame and with a crystal-to-detector distance of 5 cm. The unit-cell parameters for franconite, obtained by least-squares refinement of 19,947 reflections ( $I > 10\sigma I$ ), are  $a = 10.119(2)$ ,  $b = 6.436(1)$ ,  $c = 12.682(2)$  Å and  $\beta = 99.91(3)^\circ$  (Table 5). The original unit cell [ $a = 22.22(1)$ ,  $b = 12.857(5)$ ,  $c = 6.359(4)$  Å and  $\beta = 92.24(6)^\circ$ ] determined by Jambor *et al.* (1984) was obtained by electron diffraction and indexing of an XRPD pattern; as a result the weak reflections supporting the halving of the unit cell along the  $a$  axis may have been missed. An empirical absorption correction (SADABS; Sheldrick, 1997) was applied and equivalent reflections merged to give 28,634 unique reflections covering the entire Ewald sphere.

Solution and refinement of the crystal structure of franconite were performed using *SHELXL-97* (Sheldrick, 1997). The crystal structure was solved using direct methods, using the scattering curves of Cromer and Mann (1968) and the scattering factors of Cromer and Liberman (1970). Phasing of a set of normalized structure factors gave a mean value of  $|E^2 - 1|$  of 0.912, consistent with a centre of symmetry being present  $\{|E^2 - 1| = 0.968$  for centrosymmetric and  $|E^2 - 1| = 0.736$  for non-centrosymmetric}. Based on this and the space-group choices available,  $P2_1/c$  (#14) was chosen as the correct space group. Phase-normalized structure factors were used to give a Fourier difference map from which two  $Nb$  and several  $O$  sites were located.

The  $Na$  site and additional  $O$  sites were identified from subsequent Fourier difference maps. Refinement of the site-occupancy factors (SOF) indicated that all of the cation and anion sites were fully occupied (Table 6). Determination of which  $O$  sites were occupied by OH or  $H_2O$  was based on bond-valence calculations and electro-neutrality considerations (Table 7). During the later stages of refinement, seven  $H$  sites were located in the difference Fourier maps. These were inserted into the refinement with H–O distances being constrained to be close to 0.98 Å. Refinement of this model converged to  $R = 4.63\%$  and  $wR^2 = 11.95\%$ .

## Description of crystal structure

### Cation polyhedra

The crystal structure of franconite has one [5]-coordinated  $Na$  site bonded to four  $H_2O$  groups and a single  $O$  atom, producing an  $NaO(H_2O)_4$  polyhedron. This is unusual in rock-forming minerals, in that  $Na$  typically occurs in [6] or higher. However, in rare instances it can occur in [5] as in zeravshanite [ $Cs_4Na_2Zr_3(Si_{18}O_{45})(H_2O)_2$ ; Uvarova *et al.*, 2004] and mejillonesite [ $NaMg_2(PO_3OH)(PO_4)(OH)\cdot H_5O_2$ ; Atencio *et al.*, 2012] and even as low as [4], as in vuonnemite [ $(Na_{11}TiNb_2(Si_2O_7)_2(PO_4)_2O_3(F,OH)$ ; Ercit *et al.*, 1998)]. Average Na–O bond lengths in zeravshanite and mejillonesite are 2.400 and 2.396 Å, respectively, with bond lengths for both minerals ranging from 2.275(5) to 2.615(4) Å. In franconite, Na–(O, $H_2O$ ) bond lengths range from 2.337(6) to 2.422(7) Å with an average bond length of 2.390 Å (Table 8), in good agreement with those observed for  $^{23}Na$  in zeravshanite and mejillonesite.

TABLE 5. Miscellaneous data for franconite.

$a$ (Å)	10.119(2)	Monochromator	Graphite
$b$ (Å)	6.436(1)	Intensity-data collection	0:20
$c$ (Å)	12.682(2)	Criterion for observed reflections	$F > 4\sigma(F)$
$\beta$ (°)	99.91(3)	Goof	1.022
$V$ (Å <sup>3</sup> )	813.6	Total No. of reflections	28653
Space Group	$P2_1/c$ (#14)	No. Unique reflections	2380
$Z$	4	$R$ (merge %)	5.93
Radiation	Mo $K\alpha$ (50 kV, 40 mA)	$R$ %	4.63
		$wR^2$ %	11.95

TABLE 6. Atomic positions and displacement parameters ( $\text{\AA}^2$ ) for franconite.

Atom	$x$	$y$	$z$	$U^{11}$	$U^{22}$	$U^{33}$	$U^{23}$	$U^{13}$	$U^{12}$	$U_{\text{eq}}$
Na(1)	0.5288(3)	0.2454(5)	0.3395(3)	0.032(2)	0.030(2)	0.030(2)	0.001(1)	0.008(1)	0.002(1)	0.0304(6)
Nb(1)	0.1633(5)	0.2742(8)	0.40382(4)	0.0198(3)	0.0071(2)	0.0099(2)	0.0003(2)	0.0043(2)	0.0001(2)	0.0120(1)
Nb(2)	-0.00108(5)	0.18674(7)	0.60733(4)	0.0228(3)	0.0057(2)	0.0076(2)	-0.0006(2)	0.0045(2)	0.0001(2)	0.0119(1)
O(1)	0.1710(4)	0.2516(6)	0.5586(3)	0.021(2)	0.011(2)	0.012(2)	0.001(1)	0.003(2)	0.000(2)	0.0147(8)
O(2)	-0.1673(4)	0.0287(7)	0.6170(3)	0.025(2)	0.011(2)	0.014(2)	0.000(1)	0.007(2)	0.001(2)	0.0160(8)
O(3)	0.0729(5)	0.1963(7)	0.7489(3)	0.035(3)	0.014(2)	0.009(2)	0.000(1)	0.004(2)	-0.001(2)	0.0191(9)
O(4)	-0.0845(5)	0.4391(6)	0.5862(3)	0.032(2)	0.006(2)	0.016(2)	0.000(1)	0.007(2)	0.003(2)	0.0179(9)
O(5)	0.3290(5)	0.3395(8)	0.3959(4)	0.024(2)	0.022(2)	0.022(2)	-0.003(2)	0.010(2)	-0.001(2)	0.0223(9)
OH(6)	0.0483(4)	-0.1383(6)	0.5714(3)	0.021(2)	0.008(2)	0.011(2)	-0.003(1)	0.002(1)	0.001(1)	0.0134(8)
OW(7)	0.7421(6)	0.3854(8)	0.3178(4)	0.035(3)	0.026(3)	0.024(2)	0.001(2)	0.009(2)	-0.008(2)	0.028(1)
OW(8)	0.6084(6)	0.2536(9)	0.5286(5)	0.031(3)	0.030(3)	0.031(3)	-0.001(2)	0.001(2)	0.002(2)	0.031(1)
OW(9)	0.4335(6)	0.378(1)	0.1641(5)	0.035(3)	0.037(3)	0.037(3)	0.003(3)	0.002(2)	-0.006(2)	0.037(1)
H(1)	0.124(5)	-0.20(1)	0.619(5)							0.01(2)
H(2)	0.78(1)	0.50(1)	0.364(8)							0.07(4)
H(3)	0.78(1)	0.41(2)	0.254(5)							0.07(4)
H(4)	0.60(1)	0.395(7)	0.553(9)							0.06(3)
H(5)	0.68(1)	0.17(2)	0.57(1)							0.11(6)
H(6)	0.347(4)	0.32(1)	0.133(6)							0.02(2)
H(7)	0.511(8)	0.37(2)	0.128(9)							0.08(4)

## CRYSTAL CHEMISTRY OF FRANCONITE

TABLE 7. Bond-valence table (v.u.) for franconite.

	Na	Nb(1)	Nb(2)	$\Sigma$	H(1)	H(2)	H(3)	H(4)	H(5)	H(6)	H(7)	$\Sigma$
O(1)		0.806 <sup>↓→</sup>	0.893 <sup>↓→</sup>	1.699		0.15 <sup>↓→</sup>				0.15 <sup>↓→</sup>		1.999
O(2)		0.812 <sup>↓→</sup>	0.857 <sup>↓→</sup>	1.669			0.15 <sup>↓→</sup>		0.17 <sup>↓→</sup>			1.989
O(3)		1.269 <sup>↓→</sup>	0.727 <sup>↓→</sup>	1.996								1.996
O(4)		1.251 <sup>↓→</sup>	0.739 <sup>↓→</sup>	1.990								1.990
O(5)	0.233 <sup>↓→</sup>		1.558 <sup>↓→</sup>	1.791				0.15 <sup>↓→</sup>				1.941
OH(6)		0.832 <sup>↓→</sup>	0.279 <sup>↓→</sup>	1.111	0.84 <sup>↓→</sup>							1.951
OW(7)	0.198 <sup>↓→</sup>			0.198	0.16 <sup>↓→</sup>	0.85 <sup>↓→</sup>	0.85 <sup>↓→</sup>					2.058
OW(8)	0.198 <sup>↓→</sup>			0.198				0.85 <sup>↓→</sup>	0.83 <sup>↓→</sup>		0.15 <sup>↓→</sup>	2.028
OW(9)	0.380 <sup>↓→</sup>			0.380						0.85 <sup>↓→</sup>	0.85 <sup>↓→</sup>	2.080
$\Sigma$	1.009	4.970	5.053		1.00	1.00	1.00	1.00	1.00	1.00	1.00	

\* Bond valences for *H* sites determined using parameters from Brown and Altermatt (1985). Bond valences for other sites were determined using parameters from Brese and O'Keeffe (1991).

TABLE 8. Interatomic distances (Å) in franconite.

<i>NaO(H<sub>2</sub>O)<sub>4</sub></i> Polyhedron		<i>Nb(2)O<sub>4</sub>(OH)<sub>2</sub></i> Octahedron			
<i>Na</i> –O5	2.337(6)	<i>Nb2</i> –O3	1.823(4)		
–OW8	2.396(7)	–O4	1.829(4)		
–OW7	2.398(6)	–O2	1.988(4)		
–OW9	2.399(7)	–O1	1.990(4)		
–OW9	<u>2.422(7)</u>	–OH6	2.217(4)		
< <i>Na</i> –O>	2.390	–OH6	<u>2.256(4)</u>		
		< <i>Nb2</i> –O>	2.017		
<i>Nb(1)O<sub>5</sub>(OH)</i> Octahedron					
<i>Nb1</i> –O5	1.748(5)				
–O1	1.956(4)				
–O2	1.969(4)				
–O4	2.023(4)				
–O3	2.029(4)				
–OH6	<u>2.384(4)</u>				
< <i>Nb1</i> –O>	2.018				
Hydrogen bonding					
Donor–H	<i>d</i> (D–H; Å)	<i>d</i> (H···A; Å)	<DHA (°)	<i>d</i> (D···A; Å)	Acceptor
OH6–H1	0.980	1.868	164.48	2.824	OW7
OW7–H2	0.980	1.901	167.63	2.866	O1
OW7–H3	0.980	1.934	170.30	2.905	O2
OW8–H4	0.980	1.938	149.20	2.823	O5
OW8–H5	0.980	1.816	159.84	2.762	O2
OW9–H6	0.980	1.918	168.04	2.884	O1
OW9–H7	0.980	1.909	151.41	2.800	OW8

The crystal structure also contains two *Nb* sites in octahedral coordination with O atoms and OH groups: Nb(1)O<sub>5</sub>(OH) and Nb(2)O<sub>4</sub>(OH)<sub>2</sub> (Fig. 3). Both are highly distorted with Nb–(O,OH) bond lengths ranging from 1.748(5)–2.384(4) Å and 1.823(4)–2.256(4) Å, respectively (Table 8). The Nb(1)O<sub>5</sub>(OH) octahedron has four equatorial bond lengths of ~2 Å as well as two asymmetrical apical bonds: a short one of 1.746(5) Å and a long one of 2.383(4) Å, the former possibly representing a Nb–O double bond (Jehng and Wachs, 1990). This type of octahedron is unusual in naturally occurring minerals; however, similar octahedra are known to occur in nenadkevichite (Rastsvetaeva *et al.*, 1994), vuonnemite (Ercit *et al.*, 1998), epistolite (Sokolova and Hawthorne, 2004) and laurentianite (Haring *et al.*, 2012). The Nb(2)O<sub>4</sub>(OH)<sub>2</sub> octahedron has three pairs of equivalent bonds: two short bonds with lengths of 1.823(4) and 1.829(4) Å, two long bonds with lengths of 2.217(4) and 2.256(4) Å and two bonds of intermediate lengths of 1.988(4) and 1.990(4) Å. This second type of octahedra is very rare in naturally occurring minerals and has only been reported in nacareniobsite-(Ce) [Na<sub>3</sub>Ca<sub>3</sub>REENb(Si<sub>2</sub>O<sub>7</sub>)<sub>2</sub>OF<sub>3</sub>; Sokolova and Hawthorne, 2008]. In both Nbφ<sub>6</sub> (φ = O, OH, H<sub>2</sub>O) octahedra, the longest bond lengths correspond to Nb–OH bonds whereas the shortest bond lengths correspond to Nb–O bonds, the short distances probably reflecting the presence of double bonds. When in octahedral coordination, small highly charged cations such as Nb<sup>5+</sup> often cause significant O–O repulsion which leads to strain on O–M–O bonds (Megaw, 1968*a,b*). To reduce this strain, the Nb<sup>5+</sup> cation will undergo an off-

centre displacement resulting in distorted octahedra with large ranges in bond length. These large ranges in Nb–(O,OH) bond length are consistent with those observed in the Nb(O,OH)<sub>6</sub> present in the crystal structure of franconite.

### Bond topology

The limited number of cation polyhedra present constrains the bond topology in franconite to being relatively simple. First, the Nb(1)O<sub>5</sub>(OH) and Nb(2)O<sub>4</sub>(OH)<sub>2</sub> octahedra are linked through shared edges to form four-membered clusters consisting of two Nb(1)O<sub>5</sub>(OH) and two Nb(2)O<sub>4</sub>(OH)<sub>2</sub> octahedra (Fig. 4). Each four-membered Nb(O,OH)<sub>6</sub> cluster is subsequently linked to six adjacent clusters through shared corners, thus forming infinite sheets parallel to [100] (Fig. 4). This strongly affects the morphology of the crystals, which are platy and flattened on {100}. The Na(O,H<sub>2</sub>O)<sub>5</sub> polyhedra are linked through shared corners to form single chains parallel to [100] (Fig. 5). These chains of NaO(H<sub>2</sub>O)<sub>4</sub> polyhedra form distinct layers which alternate with layers of Nb(O,OH)<sub>6</sub> octahedra along [100]. Each NaO(H<sub>2</sub>O)<sub>4</sub> polyhedral layer is weakly linked to sheets of Nb(O,OH)<sub>6</sub> octahedra through shared O(5) anions and more importantly H bonds (Fig. 6), which are discussed below.

### Hydrogen bonding

The crystal structure of franconite is quite interesting in light of the well defined H bonding that is essential to completing the crystal structure. There are three H<sub>2</sub>O groups [OW(7), OW(8) and OW(9)] and one OH [OH(6)]

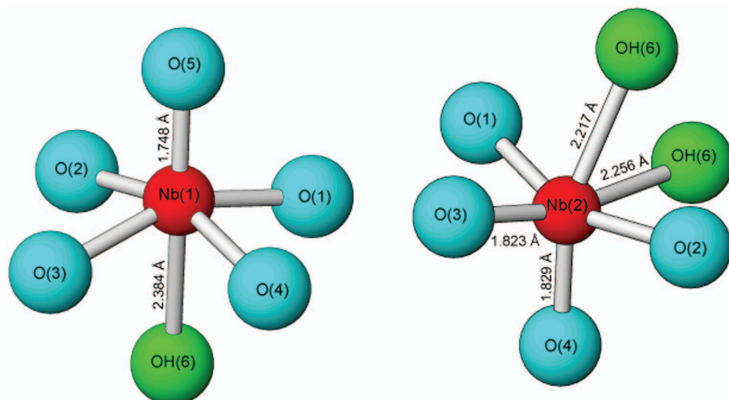


FIG. 3. The two distorted octahedral *Nb* sites in franconite.

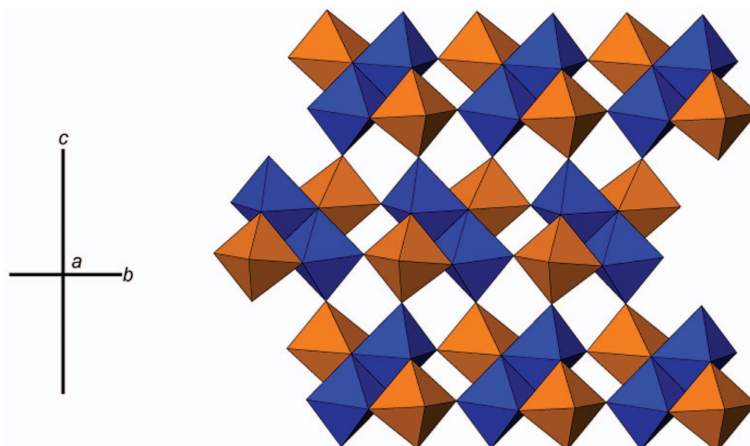


FIG. 4. Octahedral layer in franconite consisting of Nb(1)O<sub>5</sub>(OH) octahedra (dark blue) and Nb(2)O<sub>4</sub>(OH)<sub>2</sub> octahedra (orange).

group present in the crystal structure. The H bonds associated with the OH and H<sub>2</sub>O groups are separated into two groups: (1) those within Na–Nb polyhedral layers and (2) those between the Na–Nb polyhedral layers. The first group of H bonds are restricted to the NaO(H<sub>2</sub>O)<sub>4</sub> polyhedral layer. These involve H(4) and H(7) that are bonded to the OW(8) and OW(9) groups, respectively and project towards adjacent chains of NaO(H<sub>2</sub>O)<sub>4</sub> polyhedra (Fig. 7). Each H(4) is located ~1.94 Å from O(5) atoms while each H(7) is located ~1.91 Å from OW8 groups generating H bonds between adjacent NaO(H<sub>2</sub>O)<sub>4</sub> polyhedral chains within the NaO(H<sub>2</sub>O)<sub>4</sub> polyhedral layer.

The second group, which includes three sets of H bonds, occur between layers of NaO(H<sub>2</sub>O)<sub>4</sub> polyhedra and Nb(O,OH)<sub>6</sub> octahedra. The bonds in each set share similar orientations with respect to one another. The first set involves H(1) that is bonded to OH(6) [coordinated with Nb(O,OH)<sub>6</sub> octahedra]. Each H(1) projects towards the

NaO(H<sub>2</sub>O)<sub>4</sub> polyhedral layer and is located ~1.87 Å from OW7 [coordinated with NaO(H<sub>2</sub>O)<sub>4</sub> polyhedra], forming a H bond between the Nb(O,OH)<sub>6</sub> octahedral layer and the NaO(H<sub>2</sub>O)<sub>4</sub> polyhedral layer (Fig. 8a). The second set of H bonds involves H(2) and H(3) that are bonded to OW(7), both projecting towards the Nb(O,OH)<sub>6</sub> octahedral layer. Each H(2) is located ~1.90 Å from O(1) atoms while each H(3) is located ~1.93 Å from O2, generating additional H bonds between the NaO(H<sub>2</sub>O)<sub>4</sub> and Nb(O,OH)<sub>6</sub> layers (Fig. 8b). The third set of interlayer H bonds involves H(5) and H(6) that are bonded to OW(8) and OW(9) groups, respectively. Both H(5) and H(6) project from the NaO(H<sub>2</sub>O)<sub>4</sub> layers towards the Nb(O,OH)<sub>6</sub> layers. Each H(5) is located ~1.82 Å from O(2) atoms while H(6) is located ~1.92 Å from O(1), both generating the remaining H bonds between the NaO(H<sub>2</sub>O)<sub>4</sub> and Nb(O,OH)<sub>6</sub> layers (Fig. 8c). The second group of interlayer H bonds involve

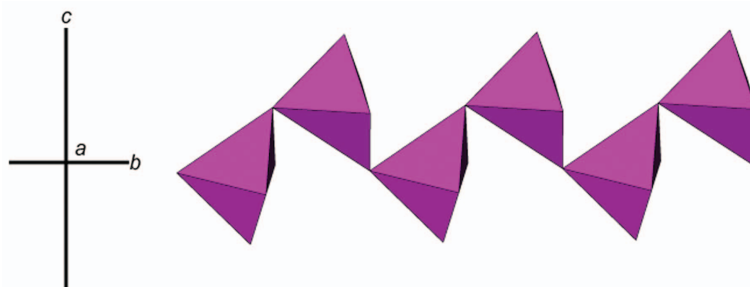


FIG. 5. Chains of edge-sharing NaO(H<sub>2</sub>O)<sub>4</sub> polyhedra parallel to [100]

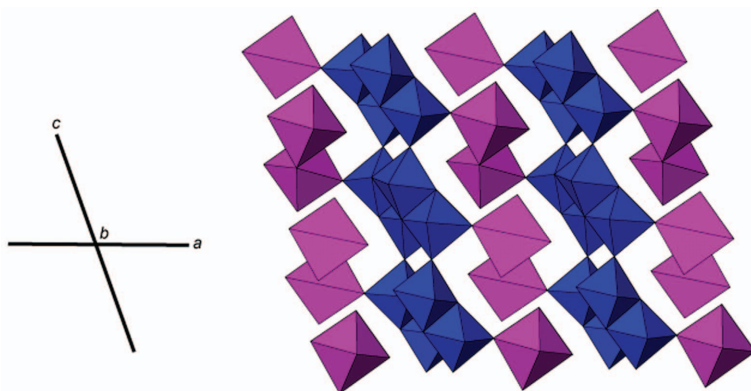


FIG. 6. The crystal structure of franconite projected onto [010] showing layers of  $\text{NbO}_6$  octahedra (dark blue) alternating with layers containing  $\text{NaO}(\text{H}_2\text{O})_4$  polyhedra (pink).

H(1), H(2), H(3), H(5) and H(6) and these play a critical role in the crystal structure of franconite. The predominance of H bonding serves to link the  $\text{Na}(\text{O}, \text{H}_2\text{O})_5$  and  $\text{Nb}(\text{O}, \text{OH})_6$  layers, thereby completing the crystal structure of the mineral and also leads to the perfect [100] cleavage observed in franconite.

### Related structures

The crystal structure of franconite is broadly similar to those of the synthetic compounds  $\text{Na}_2\text{Nb}_4\text{O}_{11}$  (Masó *et al.*, 2011) and  $\text{KCa}_2\text{Nb}_3\text{O}_{10}$  (Fukoka *et al.*, 2000, Jehng and Wachs, 1990) as well as SOMS (Nyman *et al.*, 2001, 2002). Both  $\text{Na}_2\text{Nb}_4\text{O}_{11}$  and  $\text{KCa}_2\text{Nb}_3\text{O}_{10}$  have been synthesized at high  $T$  ( $\sim 1100$ – $1300^\circ\text{C}$ ) and have distinct ferroelectric and dielectric properties, making them useful in constructing

ferroelectric capacitors (Masó *et al.*, 2011; Yim *et al.*, 2013). From a crystal-structure perspective, both  $\text{Na}_2\text{Nb}_4\text{O}_{11}$  and  $\text{KCa}_2\text{Nb}_3\text{O}_{10}$  are constructed of alternating Nb polyhedral and (Na, K) polyhedral layers similar to those in franconite, but with bond topologies that differ from those of franconite. Synthetic  $\text{Na}_2\text{Nb}_4\text{O}_{11}$ , like franconite, is monoclinic but it crystallizes in the space group  $C2/c$ . It has two unique Nb sites, but unlike those in franconite, one occurs as  $\text{NbO}_7$  bipyramids, with  $\langle \text{Nb}-\text{O} \rangle$  is 2.0570 Å and Nb–O bonds ranging from 1.9638(10)–2.4136(21) Å (Masó *et al.*, 2011). The second occurs as in  $\text{NbO}_6$  octahedra with six identical Nb–O bonds of 1.9943(10) Å (Masó *et al.*, 2011). The crystal structure of  $\text{Na}_2\text{Nb}_4\text{O}_{11}$  is layered, as in franconite, with layers of edge-sharing  $\text{NbO}_7$  bipyramids alternating along [001] with mixed layers containing both  $\text{NbO}_6$  octahedra and  $\text{NaO}_7$

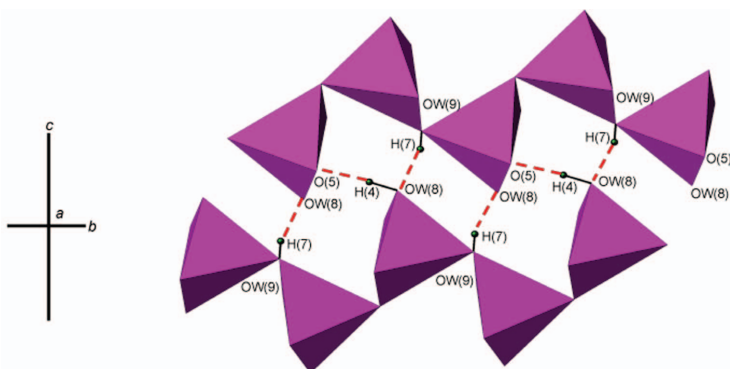


FIG. 7. The local environment of group 1 hydrogen bonds. These hydrogen bonds only occur within the  $\text{Na}(\text{O}, \text{H}_2\text{O})_5$  polyhedral layer and link together adjacent chains of  $\text{NaO}(\text{H}_2\text{O})_4$  polyhedra.

## CRYSTAL CHEMISTRY OF FRANCONITE

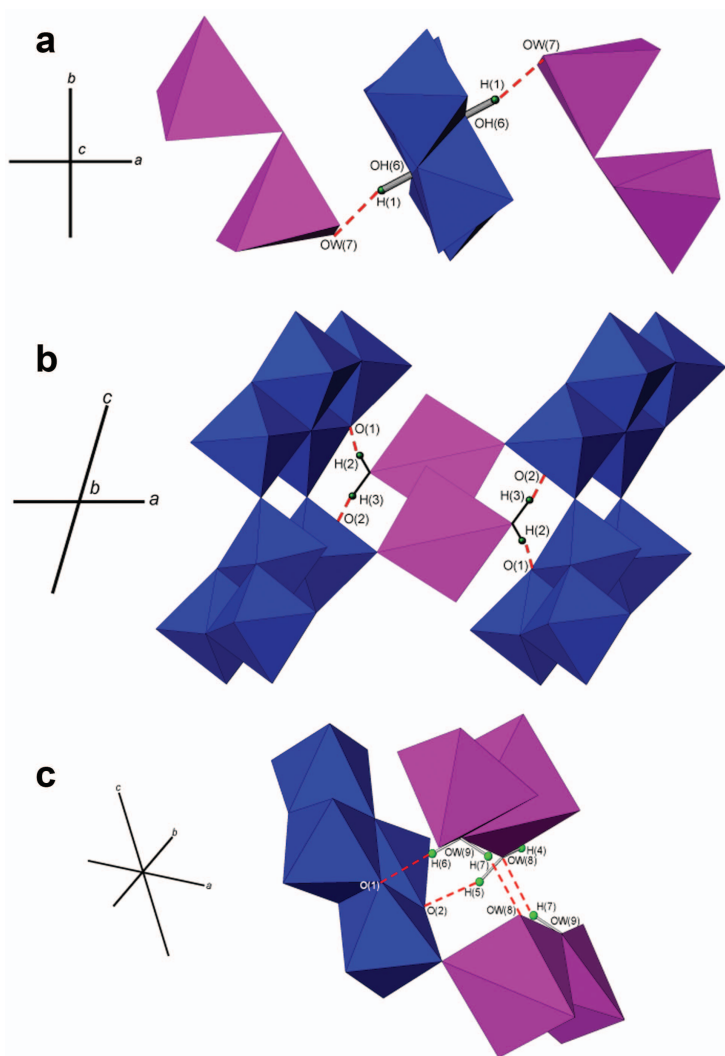


FIG. 8. The local environment of group 2 interlayer H bonds. These H bonds link together the  $\text{Na}(\text{O},\text{H}_2\text{O})_5$  polyhedral layer and  $\text{Nb}(\text{O},\text{OH})_6$  octahedral layers. Group 1 H bonds occur in three sets including (a) Set 1 involving H(1) atoms (b) Set 2 involving H(2) and H(3) atoms, and (c) Set 3 atoms involving H(5) and H(6) atoms.

polyhedra (Masó *et al.*, 2011). This differs from the crystal structure of franconite where the  $\text{Nb}(\text{O},\text{OH})_6$  octahedra and  $\text{NaO}(\text{H}_2\text{O})_5$  polyhedra occupy distinct layers within the crystal structure. The crystal structure of  $\text{KCa}_2\text{Nb}_3\text{O}_{10}$ , unlike franconite, is orthorhombic with  $Cmcm$  space-group symmetry. This compound is described as having a layered perovskite structure with distinct layers of  $^{[6]}\text{Nb}$ . There are two Nb sites in the crystal structure, both being [6]-coordinated by O in  $\text{NbO}_6$  octahedra, rather than the  $\text{Nb}(\text{O},\text{OH})_6$

octahedra found in franconite. The Nb sites in  $\text{KCa}_2\text{Nb}_3\text{O}_{10}$  have Nb–O bond lengths similar to those observed in franconite. The first is similar to the  $\text{Nb}(2)\text{O}_4(\text{OH})_2$  octahedron in franconite, with three pairs of equivalent bonds: two short bonds both with lengths of 1.989(3) Å, two long bonds both with lengths of 2.024(4) Å and two bonds with an intermediate length of 1.905(7) Å (Fukoka *et al.*, 2000). The second is similar to the  $\text{Nb}(1)\text{O}_5(\text{OH})$  octahedron in franconite, consisting of a short Nb–O bond of 1.748(6) Å,

a long Nb–O bond of 2.389(7) Å, as well as four equatorial bonds (Fukoka *et al.*, 2000). Furthermore, the NbO<sub>6</sub> octahedral layers in KCa<sub>2</sub>Nb<sub>3</sub>O<sub>10</sub> are the result of NbO<sub>6</sub> octahedra linked to adjacent NbO<sub>6</sub> octahedra through shared corners. These layers of NbO<sub>6</sub> layers contain interstitial Ca<sup>2+</sup> cations and alternate with layers of KO<sub>7</sub> polyhedra (Fukoka *et al.*, 2000).

SOMS, unlike Na<sub>2</sub>Nb<sub>4</sub>O<sub>11</sub> and KCa<sub>2</sub>Nb<sub>3</sub>O<sub>10</sub>, can be synthesized at low temperatures (*T* ~175°C) under alkaline conditions (pH ~13.7; Xu *et al.*, 2004). Franconite is expected to have formed under similar conditions based on its hydrous crystal structure (see discussion below) and association with carbonate minerals such as siderite and calcite (this study; Jambor *et al.*, 1984). SOMS exhibit a strong ion-exchange selectivity for divalent cations over monovalent cations making them useful in removing heavy metals such as Pb<sup>2+</sup>, Co<sup>2+</sup> and Cd<sup>2+</sup> from ground water and soils (Nyman *et al.*, 2001). Nb-dominant SOMS [Na<sub>2</sub>Nb<sub>2</sub>O<sub>6</sub>·H<sub>2</sub>O; Nyman *et al.*, 2001] are hydrated and have crystal structures with cation ratios similar to those of franconite. The crystal structure of Nb-dominant SOMS, like franconite, is monoclinic but it crystallizes in the space group *C2/c* (Nyman *et al.*, 2001). It consists of sheets of edge-sharing Na(O,H<sub>2</sub>O)<sub>6</sub> octahedra (Nyman *et al.*, 2001) instead of chains of corner sharing Na(O,H<sub>2</sub>O)<sub>5</sub> polyhedra, as is observed in franconite. These sheets of edge-sharing Na(O,H<sub>2</sub>O)<sub>6</sub> octahedra alternate with layers containing double chains of NbO<sub>6</sub> octahedra with Na(O,H<sub>2</sub>O)<sub>4</sub> polyhedra (Nyman *et al.*, 2001) occurring between the double chains. The

NbO<sub>6</sub> sites in SOMS, are similar to the Nb(1)O<sub>5</sub>(OH) sites in franconite, with a short apical bond of ~1.8 Å and a long one of ~2.4 Å as well as four equatorial bonds with distances of ~2 Å (Nyman *et al.*, 2002).

Although their crystal structures have not yet been determined, those of ternovite and hochelagaite are expected to be related to that of franconite based on the similarity of their XRPD patterns and cationic ratios. This implies that, despite differences in chemistry amongst the three minerals, the structure type that is common to all three must be considered to be highly flexible, at least in terms of the alkalis and alkaline-earths that may be accommodated. Chemical data from franconite, hochelagaite and ternovite (Fig. 9) indicate that a nearly complete solid solution exists between franconite and hochelagaite; if one assumes similar stoichiometries for the two, The Ca-Na substitution presumably involves the generation of vacancies or the conversion of O to OH (e.g. Ti<sup>4+</sup> + OH<sup>-</sup> ↔ Nb<sup>5+</sup> + O<sup>2-</sup> substitution in SOMS; Nyman *et al.*, 2001) in order to maintain charge-balance. In the crystal-structure refinement of franconite, the *O* and *OH* sites were found to be fully occupied. Furthermore, chemical data (*n* = 35) from five franconite-rich globules show a strong, inverse ~2:1 correlation between Na and Ca in terms of atoms per formula unit (a.p.f.u.) (Fig. 10), while similar trends involving substitutions with other elements (e.g. Nb, Ti, Al and Si) are not evident. As such, it is probable that the Na-Ca substitution is a coupled substitution linked to the creation of vacancies, i.e. 2Na<sup>+</sup> ↔

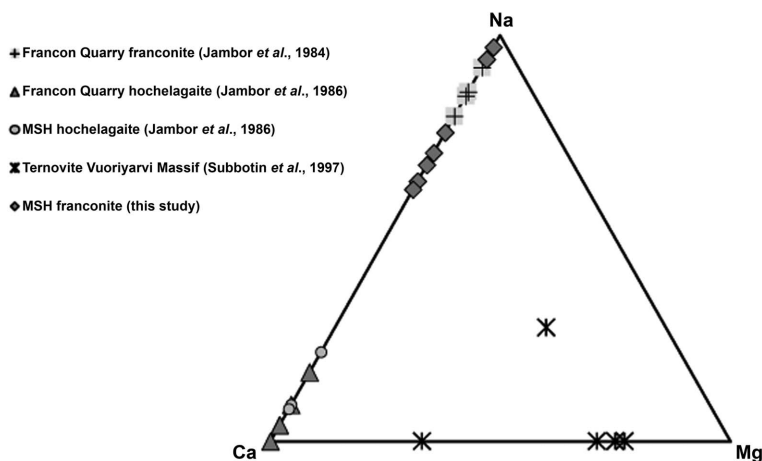


FIG. 9. Na–Ca–Mg ternary system for franconite, hochelagaite and ternovite.

## CRYSTAL CHEMISTRY OF FRANCONITE

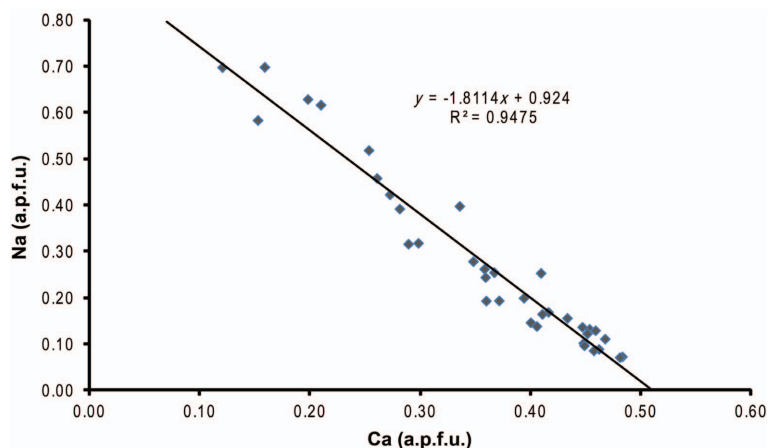


FIG. 10. Na vs. Ca content in the crystal structure of franconite. Values of Na and Ca are expressed as atoms per formula unit (a.p.f.u.)

Ca<sup>2+</sup> + □. From preliminary studies, it also appears that the unidentified mineral UK56 (Chao *et al.*, 1990) [(Ca<sub>0.5</sub>□<sub>0.5</sub>)Nb<sub>2</sub>O<sub>5</sub>(OH)·4H<sub>2</sub>O] has a crystal structure and bond topology very similar to that of franconite. In this mineral, vacancies due to Ca-Na substitution are observed where the alkali/alkali-earth site is only half-occupied by Ca instead of being fully occupied by Na as in franconite (*unpub. data*). An analysis of the chemical data available for minerals of the franconite–hochelagaite–ternovite ternary system indicates limited substitution of Mg<sup>2+</sup> and Ca<sup>2+</sup>. While the radii for <sup>[6]</sup>Ca<sup>2+</sup> (1.00 Å) and <sup>[6]</sup>Mg<sup>2+</sup> (0.72 Å) (Shannon, 1976) suggest that any Ca ↔ Mg substitution should be limited on an ionic-radius basis, the true extent of this substitution is not known, primarily due to the paucity of data related to the chemistry of ternovite. Since the crystal structures of ternovite, hochelagaite and franconite are expected to be related, the presence of ternovite containing both Ca<sup>2+</sup> and Mg<sup>2+</sup> further supports the flexibility of the franconite structure. Given the difference in ionic radii between <sup>[6]</sup>Na<sup>+</sup> (1.02 Å) and <sup>[6]</sup>Mg<sup>2+</sup> (0.72 Å), as well as the charge difference, substitution between Na<sup>+</sup> and Mg<sup>2+</sup> would likely be very limited. Although such a substitution is indicated on the franconite–hochelagaite–ternovite ternary, it is only supported by a single data point representing a Na–Mg–Ca solid solution, thus the true extent of Na ↔ Mg substitution in franconite remains uncertain. When considering the crystal-chemical flexibility of the structure type that is common to franconite, hochelagaite and ternovite, it is

more probable that the composition of the individual phase that crystallizes is most dependent on the composition of the fluids from which it is crystallizing. As such, the potential for Fe<sup>2+</sup>- as well as K<sup>+</sup>-rich compositions of franconite must be considered high.

The crystal structure of franconite is also highly flexible with respect to water content. Electron microprobe data from franconite used in this study indicate a calculated water content of 16.31 wt.%, compared to the water content of ~10–14 wt.% for franconite determined by Jambor *et al.* (1984). As water loss can occur under the vacuum conditions used for microprobe analysis, Jambor *et al.*, (1984) also measured the water content of franconite using a thermal analyzer. The results indicate that franconite can accommodate from three H<sub>2</sub>O groups under dry conditions to 26 H<sub>2</sub>O groups under humid conditions (Jambor *et al.*, 1984). This wide variation in H<sub>2</sub>O content suggests that H<sub>2</sub>O in franconite can be either structurally bound or loosely bound, possibly adhering to the large surface areas present in franconite, not unlike the situation for many clays (Salles *et al.*, 2009; Barshad, 1952). Results indicate that the loosely bound water is readily expelled under dry or vacuum conditions, whereas part of the structurally bound water is released upon heating to 110°C with the remainder being released upon heating to 356°C (Jambor *et al.*, 1984). The loss of the structurally bound water in franconite leads to a collapse in the crystal structure, as evidenced by the degradation of XRPD data collected on materials heated at 150, 250, 350 and 500°C (Jambor *et al.*, 1984). The phases present in X-ray

patterns collected at 150, 250 and 350°C could not be identified, but may correspond to  $\text{Na}_2\text{Nb}_4\text{O}_{11}(\text{H}_2\text{O})_n$  ( $n = 1$ ; Jambor *et al.*, 1984). Upon heating samples of franconite to 500°C, X-ray patterns were found to be consistent with  $\text{Na}_2\text{Nb}_4\text{O}_{11}$  (Jambor *et al.*, 1984). Hydrogen bonds involving structurally bound water are essential in stabilizing the crystal structure of franconite. The structural collapse of the crystal structure of franconite at  $T$  as low as 150°C, can probably be ascribed to the loss of H bonds resulting from the loss of structurally bound water. This structural collapse may possibly begin at temperatures as low as 110°C, as the release of structurally bound water starts at such  $T$ . Given the essential role of water in the crystal structure of franconite, it is likely that this mineral precipitated from aqueous fluids at low temperatures, <110°C. This is consistent with fluid inclusion studies by Schilling *et al.* (2011) that indicate the presence of late-stage fluids at Mont-Saint Hilaire that were trapped at temperatures lower than 340°C.

## Acknowledgements

The authors thank F.C. Hawthorne (Department of Geological Sciences, University of Manitoba) for providing access to the four-circle diffractometer and Mark C. Cooper for providing assistance with the single-crystal XRD data collection. They also thank F.C. Hawthorne and Mark C. Cooper for providing access to the electron microprobe and the University of Manitoba and Ravinder Sidhu for providing assistance with the chemical analysis. In addition Dr Joy Gray-Munro (Department of Chemistry and Biochemistry, Laurentian University) is thanked for providing access to the infrared spectrometer as well as assistance with data collection. The authors also acknowledge the comments made by Peter Leverett and an anonymous referee as well as those of the editorial board member, Ed Grew. Financial support for this research was provided through a grant to AMM from the Natural Sciences and Engineering Research Council as well as an Alexander Graham Bell Canada Graduate Scholarship to MMMH also from the Natural Sciences and Engineering Research Council.

## References

Atencio, D., Chukanov, N.V., Nestola, F., Witzke, T., Coutinho, J.M.V., Zadov, A.E., Filho, R.R.C. and

- Färber, G. (2012) Mejillonesite, a new acid sodium, magnesium phosphate mineral, from Mejillones Antofagasta, Chile. *American Mineralogist*, **97**, 19–25.
- Babechuk, M.G. and Kamber, B.S. (2011) An estimate of 1.9 Ga mantle depletion using the high-field-strength elements and Nd–Pb isotopes of ocean floor basalts, Flin Flon Belt, Canada. *Precambrian Research*, **189**, 114–139.
- Barshad, I. (1952) Adsorptive and swelling properties of clay-water system. *Clays and Clay Minerals*, **1**, 70–77.
- Belovitskaya, Y.V. and Pekov, I.V. (2004) Genetic mineralogy of the burbankite group. *New Data on Minerals*, **39**, 50–64.
- Brese, N.E. and O’Keefe, M. (1991) Bond-valence parameters for solids. *Acta Crystallographica*, **B47**, 192–197.
- Brown, I.D. and Altermatt, D. (1985) Bond-valence parameters obtained from a systematic analysis of the inorganic crystal structure database. *Acta Crystallographica*, **B41**, 244–247.
- Chao, G.Y., Conlon, R.P. and Velthuisen, J. (1990) Mont Saint-Hilaire unknowns. *The Mineralogical Record*, **21**, 363–368.
- Cooper, M.A. and Hawthorne F.C. (2012) The crystal structure of kraisslite,  $^{44}\text{Zn}_3(\text{Mn,Mg})_{25}(\text{Fe}^{3+},\text{Al})(\text{As}^{3+}\text{O}_3)_2[(\text{Si},\text{As}^{5+})\text{O}_4]_{10}(\text{OH})_{16}$ , from Sterling Hill mine, Ogdensburg, Sussex County, New Jersey, USA. *Mineralogical Magazine*, **76**, 2819–2836.
- Cromer, D.T. and Mann, J.B. (1968) X-ray scattering factors computed from numerical Hartree-Fock wave functions. *Acta Crystallographica*, **A24**, 321–324.
- Cromer, D.T. and Liberman, D. (1970) Relativistic calculation of anomalous scattering factors for X rays. *Journal of Physics and Chemistry*, **53**, 1891–1898.
- Dowty, E. (2002) *CRYSCON for Windows and Macintosh Version 1.1*. Shape Software Kingsport, Tennessee, USA.
- Ercit, T.S., Cooper, M.A. and Hawthorne, F.C. (1998) The crystal structure of vuonnemite,  $\text{Na}_{11}\text{Ti}^{4+}\text{Nb}_2(\text{Si}_2\text{O}_7)_2(\text{PO}_4)_2\text{O}_3(\text{F},\text{OH})$ , a phosphate-bearing sorosilicate of the lomonosovite group. *The Canadian Mineralogist*, **36**, 1311–1320.
- Fielicke, A., Meijer, G. and Von Helden, G. (2003) Infrared spectroscopy of niobium oxide cluster cations in a molecular beam: identifying the cluster structures. *Journal of the American Chemical Society*, **125**, 3659–3667.
- Fukoka, H., Isami, T. and Yamanaka, S. (2000) Crystal structure of a layered perovskite niobate  $\text{KCa}_2\text{Nb}_3\text{O}_{10}$ . *Journal of Solid State Chemistry*, **151**, 40–45.
- Haring, M.M.M., McDonald, A.M., Cooper, M.A. and Poirier, G.A. (2012) Laurentianite,  $[\text{NbO}(\text{H}_2\text{O})_3(\text{Si}_2\text{O}_7)_2[\text{Na}(\text{H}_2\text{O})_2]_3]$ , a new mineral from Mont

- Saint-Hilaire, Québec: description, crystal-structure determination and paragenesis. *The Canadian Mineralogist*, **50**, 1265–1280.
- Horváth, L. and Gault, R.A. (1990) The mineralogy of Mont Saint-Hilaire Québec. *The Mineralogical Record*, **21**, 284–359.
- Horváth, L., Pfenninger-Horváth, E., Gault, R.A. and Tarassoff, P. (1998) Mineralogy of the Saint-Amable Sill, Varennes and Saint-Amable, Québec. *The Mineralogical Record*, **29**, 83–118.
- Iliev, M., Phillips, M.L.F., Meen, J.K. and Nenoff, T.M. (2003) Raman spectroscopy  $\text{Na}_2\text{Nb}_2\text{O}_6\cdot\text{H}_2\text{O}$  and  $\text{Na}_2\text{Nb}_{2-x}\text{M}_x\text{O}_{6-x}(\text{OH})_x\cdot\text{H}_2\text{O}$  ( $\text{M} = \text{Ti}, \text{Hf}$ ) ion exchangers. *Journal of Physical Chemistry*, **B 107**, 14261–14264.
- Jambor, J.L., Sabina, A.P., Roberts, A.C., Bonardi, M., Ramik, R.R. and Sturman B.D. (1984) Franconite, a new hydrated Na-Nb oxide mineral from Montreal Island, Québec. *The Canadian Mineralogist*, **22**, 239–243.
- Jambor, J.L., Sabina, A.P., Roberts, A.C., Bonardi, M., Owens, D.R. and Sturman, B.D. (1986) Hochelagaite, a new calcium-niobium oxide mineral from Montreal, Québec. *The Canadian Mineralogist*, **24**, 449–453.
- Jehng, J.M. and Wachs, I.E. (1990) Structural chemistry and Raman spectra of niobium oxides. *Chemistry of Materials*, **3**, 101–107.
- Masó, N., Woodward, D.I., Várez, A. and West, A.R. (2011) Polymorphism, structural characterization and electrical properties of  $\text{Na}_2\text{Nb}_4\text{O}_{11}$ . *Journal of Material Chemistry*, **21**, 12096–12102.
- Megaw, H.D. (1968a) A simple theory of the off center displacement of cation in octahedral environment. *Acta Crystallographica*, **B24**, 149–153.
- Megaw, H.D. (1968b) The thermal expansion of interatomic bonds, illustrated by experimental evidence from niobates. *Acta Crystallographica*, **A24**, 589–604.
- Nikandrov, S.N. (1990) Franconite, first find in the USSR. *Doklady Akademii Nauk SSSR*, **305**, 700–703, [in Russian].
- Nyman, M., Tripathi, A., Parise, J.B., Maxwell, R.S., Harrison, W.T.A. and Nenoff, T.M. (2001) A new family of octahedral molecular sieves: Sodium  $\text{Ti}/\text{Zr}^{\text{IV}}$  niobates. *Journal of the American Chemical Society*, **123**, 1529–1530.
- Nyman, M., Tripathi, A., Parise, J.B., Maxwell, R.S. and Nenoff, T.M. (2002) Sandia octahedral molecular sieves (SOMS): Structural and property effects of charge-balancing the  $\text{M}^{\text{IV}}$ -substituted ( $\text{M} = \text{Ti}, \text{Zr}$ ) niobate framework. *Journal of the American Chemical Society*, **124**, 1704–1713.
- Pekov, I.V. and Podlesnyi, A.S. (2004) Kukisvumchorr deposit: Mineralogy of alkaline pegmatites and hydrothermalites. *Mineralogical Almanac*, **7**, 60–65.
- Rastsvetaeva, R.K., Tamazyán, R.A., Pushcharovsky, D.Y. and Nadezhina, T.N. (1994) Crystal structure and microtwinning of K-rich nenadkevichite. *European Journal of Mineralogy*, **6**, 503–509.
- Salles, F., Douillard, J., Denoyel, R., Bildstein, O., Jullien, M., Beurroies, I. and Damme, H. (2009) Hydration sequence of swelling clays: Evolutions of specific surface area and hydration energy. *Journal of Colloid and Interface Science*, **333**, 510–522.
- Schilling, J., Marks, M.A.W., Wenzel, T., Vennemann, T., Horváth, L., Tarassoff, P., Jacob, D.E. and Markl, G. (2011) Magmatic to hydrothermal evolution of the intrusive Mont Saint-Hilaire complex: insights into the late-stage evolution of peralkaline rocks. *Journal of Petrology*, **52**, 2147–2185.
- Shannon, R.D. (1976) Revised effective ionic radii and systematic studies in interatomic distances in halides and chalcogenides. *Acta Crystallographica*, **A32**, 751–767.
- Sheldrick, G.M. (1997) *SHELX-97: A program for crystal structure refinement*. University of Göttingen, Göttingen, Germany.
- Sokolova, E. and Hawthorne, F.C. (2004) The crystal chemistry of epistolite. *The Canadian Mineralogist*, **42**, 797–806.
- Sokolova, E. and Hawthorne, F.C. (2008) From structure topology to chemical composition. V. Titanium silicates: The crystal chemistry of nacareniobsite-(Ce). *The Canadian Mineralogist*, **46**, 1333–1342.
- Subbotin, V.V., Voloshin, A.V., Pakhomovskii, Y.A., Men'shikov, Y.P. and Subbotina, G.F. (1997) Ternovite,  $(\text{Mg}, \text{Ca})\text{Nb}_4\text{O}_{11}\cdot n\text{H}_2\text{O}$ , a new mineral and other hydrous tetranioabates from carbonatites of the Vuoriyarvi massif, Kola Peninsula, Russia. *Neues Jahrbuch für Mineralogie*, **2**, 49–60.
- Uvarova, Y.A., Sokolova, E., Hawthorne, F.C., Pautov, L.A. and Agakhanov, A.A. (2004) A novel  $[\text{Si}_{18}\text{O}_{45}]^{18-}$  sheet in the crystal structure of zervavshanite,  $\text{Cs}_4\text{Na}_2\text{Zr}_3[\text{Si}_{18}\text{O}_{45}](\text{H}_2\text{O})_2$ . *The Canadian Mineralogist*, **42**, 125–134.
- Williams, Q. (1995) Infrared, Raman and optical spectroscopy of Earth materials. Pp. 291–302 in: *Mineral Physics and Crystallography: a Handbook of Physical Constants* (T.J. Ahrens, editor), AGU Reference Shelf Vol 2. American Geophysical Union, Washington, D.C.
- Xu, H., Nyman, M., Nenoff, T.M. and Navrotsky, A. (2004) Prototype sandia octahedral molecular sieve (SOMS)  $\text{Na}_2\text{Nb}_2\text{O}_6\cdot\text{H}_2\text{O}$ : Synthesis, structure and thermodynamic stability. *Chemistry of Materials*, **16**, 2034–2040.
- Yim, H., Yoo, S., Nahm, S., Hwang, S., Yoon, S. and Choi, J. (2013) Synthesis and dielectric properties of layered  $\text{HCa}_2\text{Nb}_3\text{O}_{10}$  structure ceramics. *Ceramics International*, **39**, 611–614.